Maintenance of Quasi-Stationary Waves in a Two-Level Quasi-Geostrophic Spectral Model with Topography

MAO-SUNG YAO

Goddard Institute for Space Studies, Goddard Space Flight Center, NASA, New York, NY 10025

(Manuscript received 12 March 1979, in final form 30 July 1979)

ABSTRACT

The maintenance of the quasi-stationary waves obtained through numerically integrating a two-level quasi-geostrophic spectral model on a β-plane is studied. An idealized topography which has only wavenumber n in the zonal direction and the first mode in the meridional direction is used to force the quasi-stationary waves. However, the model's motion contains wavenumbers 0, n and $2n$ in the zonal direction, while the first three modes in the meridional direction are allowed for each wave. The cases $n = 2$ and $n = 3$ are considered.

The mechanism for maintaining the quasi-stationary waves is investigated by varying the imposed thermal equilibrium temperature gradient, ΔT_e, and the reciprocal of the internal frictional coefficient, $0.5\ k_I^{-1}$. If the flow is not highly irregular, the available potential energy of quasi-stationary waves (A_S) is maintained by the energy conversion $A_Z \rightarrow A_S$, where A_Z is the available potential energy of the time-averaged zonal mean flow. For $n = 3$ and moderately large ΔT_e and k_I^{-1}, the kinetic energy of these waves (K_S) is maintained by the energy conversion $A_S \rightarrow K_S$. If ΔT_e or k_I^{-1} is smaller while $n = 3$, kinetic energy is supplied to the quasi-stationary waves by the energy conversion $K_Z \rightarrow K_S$ through the topographic forcing, where K_Z is the kinetic energy of the time-averaged zonal mean flow. The latter mechanism also maintains the kinetic energy of the quasi-stationary waves for $n = 2$ with relatively small ΔT_e and k_I^{-1}. When ΔT_e or k_I^{-1} is sufficiently large, the flow is highly irregular and a unique regime cannot be defined for either $n = 2$ or $n = 3$.

In the case of $n = 3$ and moderately large ΔT_e and k_I^{-1}, the energy cycle, spectra and form of the quasi-stationary waves suggest that the quasi-stationary waves are largely baroclinic waves which draw their energy from the forced waves.

1. Introduction

The earth's topographical forcing is one of the major mechanisms for producing quasi-stationary waves in the atmosphere. These topographically forced waves are effective in transferring eddy energy upward into the stratosphere and mesosphere (Eliassen and Palm, 1960; Charney and Drazin, 1961; Matsuno, 1970). In addition, the topography considerably influences the angular momentum balance of the atmosphere through the mountain torque due to the pressure difference between the west and east sides of a mountain range (White, 1949; Newton, 1971). However, the mechanisms for maintaining quasi-stationary waves may be quite different from the mechanisms that force them.

Many studies have been made on the role of the topography in forcing stationary waves, such as Charney and Eliassen (1949), Bolin (1950), Gambo (1956), Murakami (1963b) and Derome and Wiin-Nielsen (1971). Most of these studies used linearized equations with prescribed zonal mean flows. Saltzman (1968) gave a general review of this kind of study.

On the other hand, there have also been some observational studies on the maintenance of the quasi-stationary component of the atmospheric circulation. Holopainen (1970) performed an observational study of the energy balance of the quasi-stationary disturbances in the Northern Hemisphere. He concluded that in winter the quasi-stationary disturbances are typically baroclinic waves which get available potential energy from the zonally averaged mean flow. These waves then convert part of their potential energy into kinetic energy to offset the loss of the latter due to small-scale turbulent friction, large-scale transient motion and conversion into zonally averaged mean motion. As far as the energy balance of the quasi-stationary waves is concerned, the effect of mountains seems to be very small. In summer the stationary disturbances appear to form a thermally driven system. In such a system conversion from available potential energy compensates for the frictional loss of kinetic energy, and the available potential energy, in turn, is maintained by generation from diabatic heating. Murakami (1963a) and Holopainen (1966) also found that the topography plays a minor role in the energy balance of quasi-stationary disturbances in the atmosphere.

Thus, it is not obvious how the theoretically calculated stationary waves are related to the observed

quasi-stationary waves. In the present study, a clear distinction is made between stationary waves, which are solutions to the governing equations without the tendency terms, and quasi-stationary waves, which are time-averaged waves. Our objective is to examine the maintenance of the quasi-stationary waves produced by a simple two-level quasi-geostrophic truncated spectral model with topography. The mechanism for maintaining the waves will depend on parameters, such as n, ΔT_e and k_I^{-1} and this dependence can be readily obtained with such a model. In Section 2, the two-level quasi-geostrophic truncated spectral model is described. In Section 3, the numerical aspects of integrating the spectral model are discussed, and the quasi-stationary solutions are compared with the stationary solutions. An analysis of the mechanisms for maintaining the quasi-stationary waves is presented in Section 4.

2. Two-level quasi-geostrophic truncated spectral model

The planetary-scale waves forced by topography and the cyclone-scale transient waves can be described by the quasi-geostrophic system of equations. We assume that the motion takes place in a cyclic zonal channel of width Y_0 in the y (meridional) direction and of a length X_0 in the x (zonal) direction. The effect of the earth's sphericity is taken into account by assuming that the Coriolis parameter has a constant meridional gradient β. Then, we have the following governing equations in p coordinates

$$\left(\frac{\partial}{\partial t} + \mathbf{v}_g\cdot\nabla\right)\zeta_g + \beta v_g - f_0\frac{\partial\omega}{\partial p} = -g\frac{\partial}{\partial p}\mathbf{k}\cdot\nabla\times\Gamma, \quad (1)$$

$$\left(\frac{\partial}{\partial t} + \mathbf{v}_g\cdot\nabla\right)\frac{\partial\phi}{\partial p} + S_p\omega = -\frac{R}{C_p p}\dot{Q}, \quad (2)$$

$$\nabla\cdot\mathbf{v} + \frac{\partial\omega}{\partial p} = 0, \quad (3)$$

$$\frac{\partial\phi}{\partial p} = -\alpha, \quad (4)$$

where t is time, p pressure, ϕ geopotential, f_0 the Coriolis parameter at a standard latitude, g gravitational acceleration, $\mathbf{k}$ a unit vector in the vertical direction, R the gas constant, C_p specific heat capacity at constant pressure, α specific volume, $\mathbf{v}$ wind velocity vector, $\omega = dp/dt$ the vertical p-velocity, $\mathbf{v}_g = f_0^{-1}\mathbf{k}\times\nabla\phi$ the geostrophic velocity, $\zeta_g = f_0^{-1}\nabla^2\phi$ the geostrophic vorticity, $S_p = -(\alpha_s/\theta_s)\times(\partial\theta_s/\partial p)$ the static stability, α_s the horizontally averaged α, θ_s the horizontally averaged potential temperature, $\Gamma = -g\rho_s^2\nu(\partial\mathbf{v}_g/\partial p)$ the frictional stress, ρ_s horizontally averaged density, ν kinematic coefficient of turbulent eddy viscosity, $\dot{Q} = -\mu C_p\times(T - T_e)$ the diabatic heating, T temperature, T_e the imposed thermal equilibrium temperature and μ a constant.

Eq. (1) is the quasi-geostrophic vorticity equation, (2) the thermodynamic equation, (3) the continuity equation and (4) the hydrostatic equation. The static stability S_p is assumed to be a constant. The diabatic heating is in the form of Newtonian cooling, where T_e is a function of y only and so does not include the thermal effect of land-sea contrast. The reciprocal of μ is the time required for the atmosphere's temperature to reach the point where $T - T_e = (T|_{t=0} - T_e)/e$ if there is no motion. We assume the following boundary conditions:

$$v_g = v = 0 \quad \text{at } Y = 0,\ Y_0$$

$$\Gamma_T = 0,\quad \omega_T = 0 \quad \text{at } P = P_T, \text{ the top of the model atmosphere,}$$

$$\Gamma_B = \rho_B C_D\mathbf{v}_g,\quad \omega_B = -\rho_B g\mathbf{v}_g\cdot\nabla h \quad \text{at the bottom of the model atmosphere,}$$

where v is the meridional wind component, C_D the drag coefficient, h the topographic function, and ρ_B a standard air density at the bottom of the atmosphere.

In the vertical direction, we divide the mass of the atmosphere into two layers. ($\Delta p = 500$ mb is used even though the surface pressure is not necessarily equal to $P_B = 1000$ mb because of the existence of topography. In other words, the topography is assumed to have a small amplitude.) As shown in Fig. 1, we carry ϕ and $\mathbf{v}$ at levels 1 and 3, ω and Γ at the top and bottom of the atmosphere, and ω, Γ and α at the middle level.

Applying Eq. (1) to levels 1 and 3, and (2) to level 2, we can derive

$$\nabla^2\frac{\partial\phi_M}{\partial t} = -\frac{1}{f_0}J(\phi_M,\nabla^2\phi_M) - \frac{1}{f_0}J(\phi_S,\nabla^2\phi_S) - \beta\frac{\partial\phi_M}{\partial x} - \epsilon J(\phi_3,h) - \frac{k_B}{2}\nabla^2\phi_B, \quad (5)$$

$$\nabla^2\frac{\partial\phi_S}{\partial t} = -\frac{1}{f_0}J(\phi_M,\nabla^2\phi_S) - \frac{1}{f_0}J(\phi_S,\nabla^2\phi_M) - \beta\frac{\partial\phi_S}{\partial x} + \epsilon J(\phi_3,h) + \frac{k_B}{2}\nabla^2\phi_B - 2k_I\nabla^2\phi_S + \frac{f_0}{\Delta p}\omega_2, \quad (6)$$

$$\frac{2}{\Delta p}\frac{\partial \phi_S}{\partial t} = -\frac{2}{f_0 \Delta p} J(\phi_M,\phi_S) + S_p\omega_2 - \frac{2\mu}{\Delta p}(\phi_S - \phi_{es}), \tag{7}$$

where

$$\left.\begin{aligned} &\phi_M = \frac{\phi_1 + \phi_3}{2}, \quad \phi_S = \frac{\phi_1 - \phi_3}{2}, \quad k_B \equiv \frac{\rho_B g C_D}{\Delta p} \\ &k_I \equiv \frac{g^2\rho_s^2\nu}{\Delta p^2}, \quad \epsilon \equiv \frac{f_0 g \rho_B}{2\Delta p}, \quad \phi_{es} = \frac{R}{2} T_{e2} \end{aligned}\right\}. \tag{8}$$

T_{e2} is the imposed thermal equilibrium temperature at level 2. Eqs. (5), (6) and (7), together with the boundary conditions, form a closed set of equations for the unknowns, ϕ_M, ϕ_S and ω_2 when other parameters are given.

In deriving (5)–(7), we let $\mathbf{v}_{g2} = (\mathbf{v}_{g1} + \mathbf{v}_{g3})/2$ and $\mathbf{v}_{gB} = (3\mathbf{v}_{g3} - \mathbf{v}_{g1})/2$. $\mathbf{v}_{g3}$, rather than $\mathbf{v}_{gB}$, is used to compute the surface vertical p-velocity in order that the topography does not make a net contribution to the time rate of change of the total energy.

We will expand the horizontal dependence of the variables in terms of double Fourier series. The techniques used are essentially those of Lorenz (1963). We denote the chosen orthogonal functions as F_1, F_2, ... They satisfy the boundary conditions and the orthogonality relations

$$\frac{1}{X_0 Y_0}\int_0^{Y_0}\int_0^{X_0} F_i F_j dxdy = \delta_{ij} \equiv \begin{cases} 1, & \text{if } i = j \\ 0, & \text{if } i \neq j. \end{cases} \tag{9}$$

The Jacobian of any two orthogonal functions will also be expanded in terms of functions F_i, such that

$$J(F_j,F_k) = \sum_{i=1}^{\infty} C_{ijk} F_i, \tag{10}$$

where the interaction coefficients C_{ijk} are computed by

$$C_{ijk} = \frac{1}{X_0 Y_0}\int_0^{Y_0}\int_0^{X_0} F_i J(F_j,F_k) dxdy. \tag{11}$$

We let ψ_i, τ_i, W_i, H_i, ψ_{Bi}, ψ_{1i}, ψ_{3i} and τ_{ei} be the spectral coefficients of variables ϕ_M, ϕ_S, ω_2, h, ϕ_B, ϕ_1, ϕ_3 and ϕ_{es}, respectively, so that

$$\phi_M = \sum_{i=1}^{\infty} \psi_i F_i, \qquad \phi_s = \sum_{i=1}^{\infty} \tau_i F_i, \text{ etc.}$$

The equations in spectral form were given by Yao (1977), and will not be shown here.

If we let $x_0 = 2\pi x/X_0$ and $y_0 = \pi y/Y_0$, the orthogonal functions F_i can be chosen to be

$$\left.\begin{aligned} \psi_{0,0} &= 1 \\ \psi_{m_0,0} &= \sqrt{2}\cos(m_0 y_0) \\ \psi_{m_0,n_0} &= 2\sin(m_0 y_0)\cos(n_0 x_0) \\ \psi'_{m_0,n_0} &= 2\sin(m_0 y_0)\sin(n_0 x_0) \end{aligned}\right\}, \tag{12}$$

where $m_0 = 1, 2, 3, \ldots, n_0 = 1, 2, 3, \ldots$.

In the results discussed in Section 4, we will restrict ourselves to some highly truncated cases where the only wavenumbers allowed are $m_0 = 1, 2$ and 3 and $n_0 = n$ and $2n$. n is the lowest existing eddy wavenumber in the x direction, as well as the wavenumber of the topography. We will describe the topography by a single component, $\psi'_{1,n}$, and the imposed thermal equilibrium temperature by two components, $\psi_{0,0}$ and $\psi_{1,0}$. Use of such a highly truncated system, with only two wavenumbers in the zonal direction allows us to see the interactions between the topographically forced stationary waves and baroclinically unstable transient waves in a most simplified form. We will only consider the cases $n = 2$ and $n = 3$, so that both topographical forcing and baroclinic instability are significant, and occur at realistic wavenumbers.

3. Numerical integration of the spectral model

The spectral model was integrated initially by perturbing the stationary solution to the equations governing the spectral coefficients. The stationary solution was obtained by the Newton method of iteration. It would be interesting to see whether there are multiple stationary solutions existing in our system as Charney and DeVore (1979) obtained in their simple barotropic system. However, since our system has 30 degrees of freedom, it is prohibitive to do so. In any case, the physical mechanisms we will study do not rely on the possibility of having multiple stationary solutions. Also we note that Yao (1977) did obtain the same stationary solution with initial guesses of no motion or stationary symmetric flows.

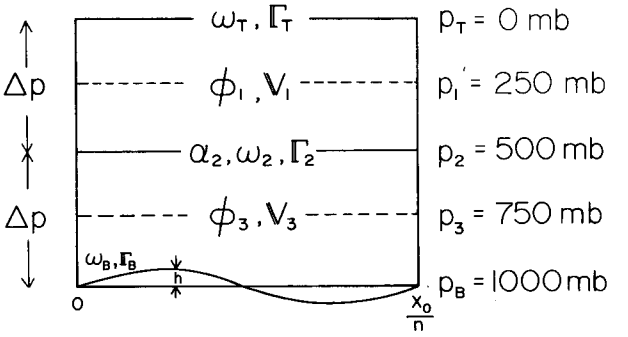

FIG. 1. Vertical discretization of the spectral model. The topographical function h is shown only for one wavelength.

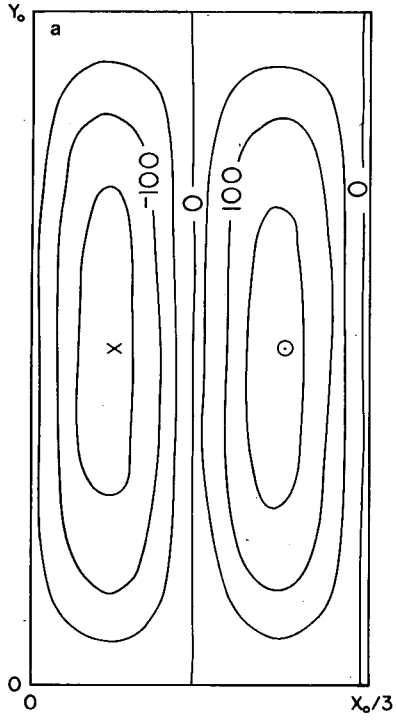

FIG. 2a. Eddy geopotential height at level 1 in the unit of m of the stationary solution with $n = 3$, $k_I^{-1} = 26$ days and $\Delta T_e = 38$ K.

Unless otherwise mentioned, we used the following parameter settings:

$X_0 = 2\pi R_e \cos 45°$, where R_e is the earth's radius

$Y_0 = 60°$ latitudinal length

$S_p = 0.03$ m^2 mb^{-2} s^{-2}

$f_0 = 10^{-4}$ s^{-1}

$\beta = 1.6 \times 10^{-11}$ m^{-1} s^{-1}

$k_B = 4k_I, \quad \mu = 2k_I.$

The amplitude of the topography is 750 m. The densities at level 2 and at the surface are based on the temperatures 250 K (T_{s2}) and 280 K (T_B), respectively. We define $\Delta T_e = T_e(0) - T_e(Y_0)$. $[T_e(0) + T_e(Y_0)]/2 = T_{s2}$.

For the earth's topography at 30°N the amplitude of the component $n = 2$ is roughly 750 m (the component $n = 3$ is generally smaller). The relations between k_I, k_B and μ are rather arbitrary. However, they provide for a bulk account of the damping effects on the atmospheric eddies, and leave ΔT_e and k_I^{-1} as parameters controlling the model's circulation properties. These damping mechanisms should also suppress some eddy energy reflected from the upper boundary. Except for the highly irregular regime, we do not expect serious distortion in the results discussed in Section 4 because of this energy reflection. Other studies (e.g., Murakami, 1963b; Derome and Wiin-Nielsen, 1971) have also used a rigid upper boundary.

In order to help us understand the physical processes discussed in Section 4, we show two sets of stationary solutions associated with $n = 3$ found by Newton's method. Figs. 2a and 2b show the eddy geopotential height at levels 1 and 3 for $k_I^{-1} = 26$ days and $\Delta T_e = 38$ K. The position labeled with a cross is the highest point of the topography and the position labeled with a circle is the lowest point of the topography. It is seen that the trough and ridge axes have very little horizontal tilt, and, therefore, the stationary waves transport only a small amount of momentum meridionally. The low geopotential center is situated slightly to the left of the ridge of the topography at level 1, while it is situated to the right at level 3. Therefore, the trough and ridge axes are tilted westward with height and it follows that heat is transported northward. The third mode in y is not so clearly seen at level 1 as it is at level 3. This might be because the wave of the third mode has a higher two-dimensional wavenumber and thus is not so effective in upward propagation as the first mode (cf. Charney and Drazin, 1961). The amplitude of the first mode is larger at level 1 than at level 3. This result is consistent with the finding by Derome and Wiin-Nielsen (1971) that the amplitude of topographically forced stationary waves of low wavenumber increases with height. The structure of the stationary waves also tells us that the moun-

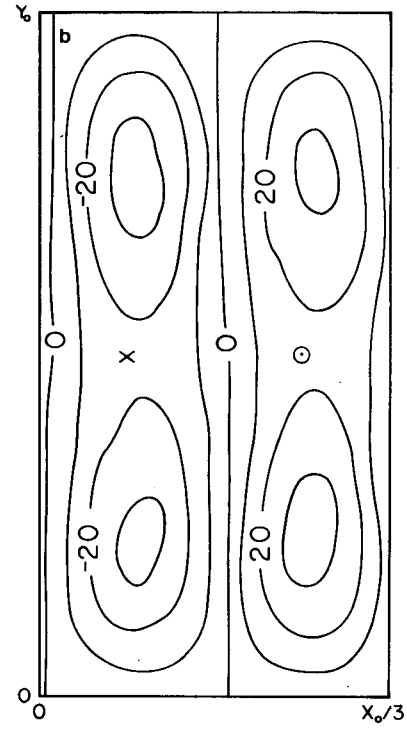

FIG. 2b. As in Fig. 2a except at level 3.

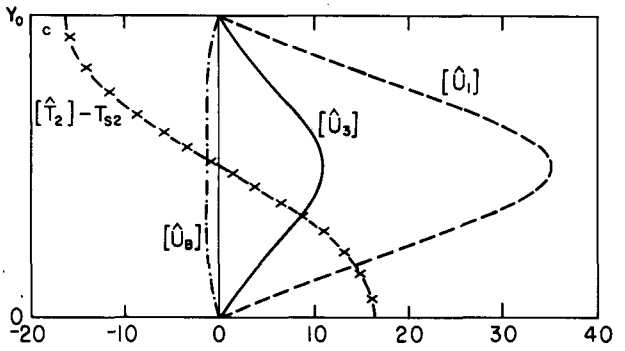

FIG. 2c. Meridional profiles of zonal mean winds (m s^{-1}) and zonal mean temperature deviation (K) from the horizontal average temperature of the stationary solution with $n = 3$, $k_I^{-1} = 26$ days and $\Delta T_e = 38$ K.

tain torque is negative and tends to drain the westerly momentum. Fig. 2c shows the meridional profiles of zonal mean winds and temperature. The surface wind is easterly and thus the frictional torque is positive and compensates for the negative mountain torque.

Figs. 3a, 3b and 3c show the corresponding fields as Figs. 2a, 2b and 2c, but with smaller ΔT_e(34 K). The general structure is similar to the case with larger ΔT_e, but the low geopotential center shifts eastward, most significantly at the middle latitudes of level 3. The amplitude of the stationary wave decreases because the zonal mean flow also decreases.

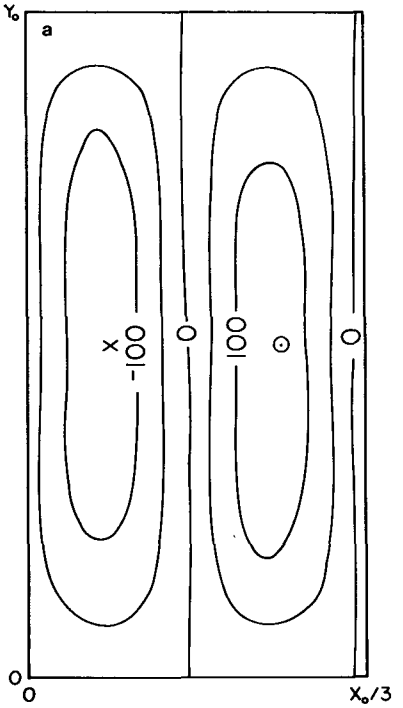

FIG. 3a. As in Fig. 2a except with $\Delta T_e = 34$ K.

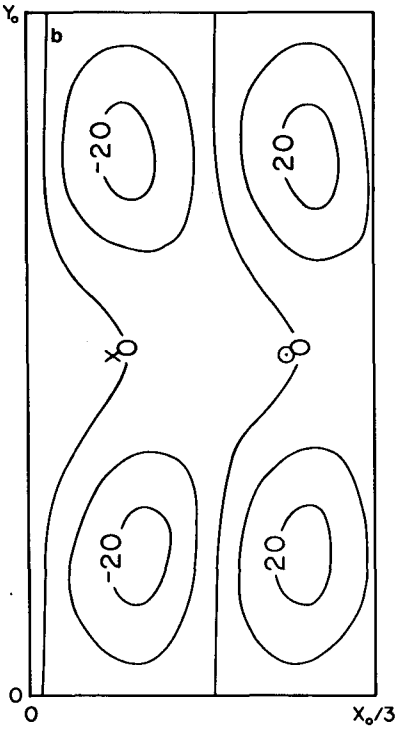

FIG. 3b. As in Fig. 2b except with $\Delta T_e = 34$ K.

Integrations were performed for periods of up to 150 days. The time step was 1 h. We used a sequence of one Matsuno step followed by five leapfrog steps. The predicted variables from days 120–150 were usually used for energetics study. The sampling frequency was once in every 6 h.

In order to compare the quasi-stationary solutions with the stationary solutions and thus help us understand the physical processes, we show the two sets of quasi-stationary solutions corresponding to Figs. 2 and 3. Figs. 4a–4c show the quasi-stationary solution with $k_I^{-1} = 26$ days and $\Delta T_e = 38$ K. When we compare this quasi-stationary solution with the corresponding stationary solution (see Figs. 2a–2c) large differences in amplitude and structure are

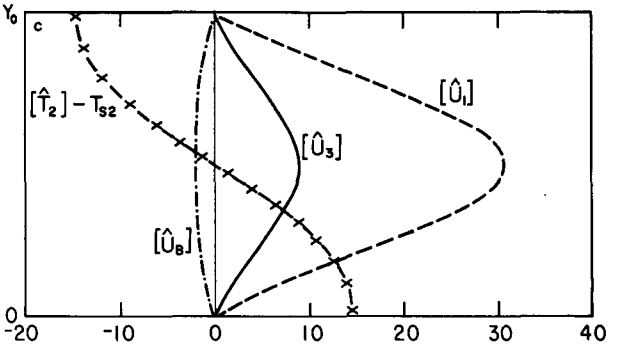

FIG. 3c. As in Fig. 2c except with $\Delta T_e = 34$ K.

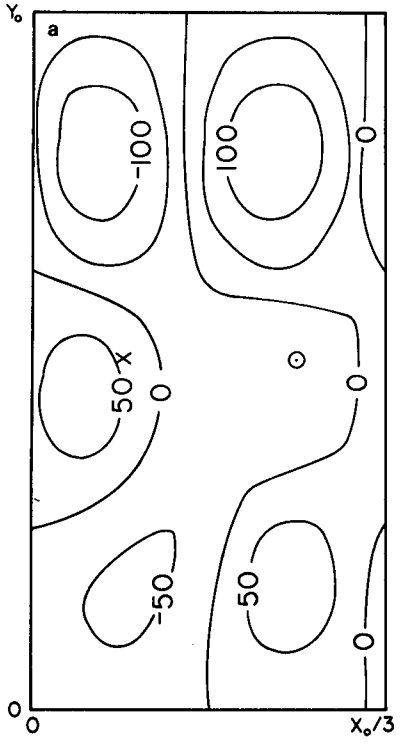

FIG. 4a. As in Fig. 2a except for the quasi-stationary solution.

noted. This suggests that the mechanism responsible for maintaining the quasi-stationary wave is quite different from the mechanism which forces them.

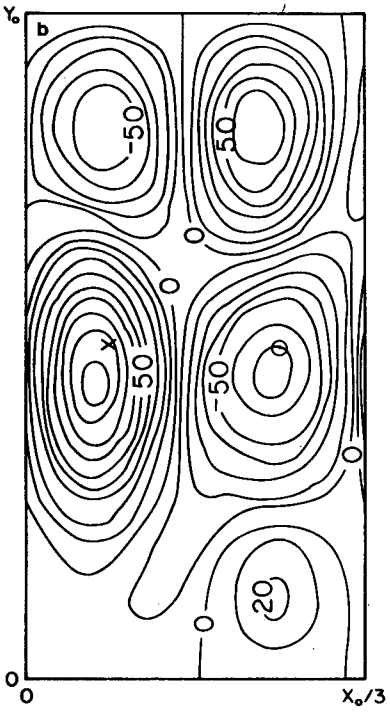

FIG. 4b. As in Fig. 2b except for the quasi-stationary solution.

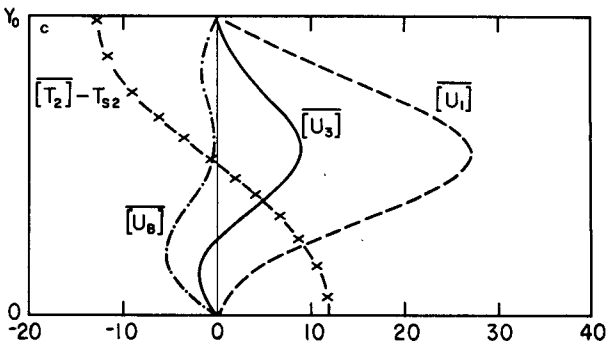

FIG. 4c. As in Fig. 2c except for the quasi-stationary solution.

However, when ΔT_e is smaller (see Figs. 5a–5c for $\Delta T_e = 34$ K) the quasi-stationary waves are quite similar to their corresponding stationary solutions. Therefore, the mechanisms maintaining the quasi-stationary waves appear to change with the parameters ΔT_e (and k_I^{-1}). Further discussion will be given in Section 4 where the energetics of the quasi-stationary solutions is presented.

4. Maintenance of quasi-stationary waves

We define the horizontally averaged kinetic energy per unit mass by

$$K = \frac{1}{X_0 Y_0} \int_0^{Y_0} \int_0^{X_0} \frac{1}{f_0^2} [(\nabla \phi_M)^2 + (\nabla \phi_S)^2] dx dy, \quad (13)$$

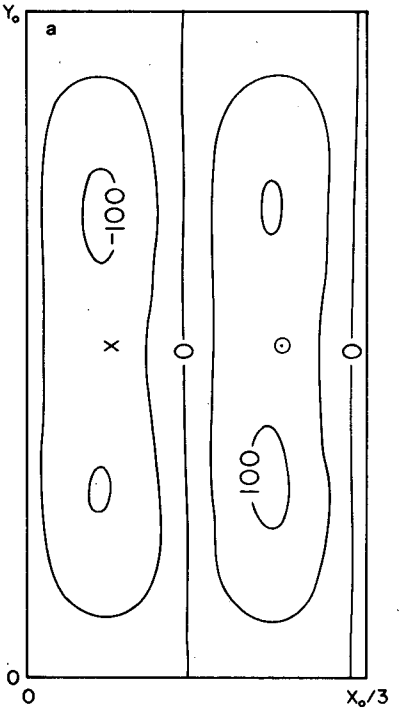

FIG. 5a. As in Fig. 3a except for the quasi-stationary solution.

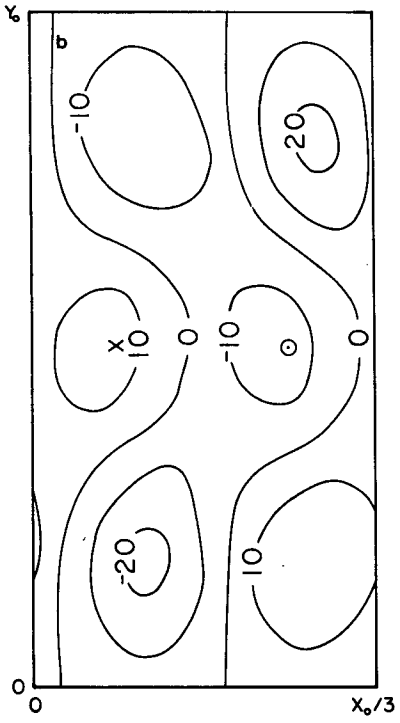

FIG. 5b. As in Fig. 3b except for the quasi-stationary solution.

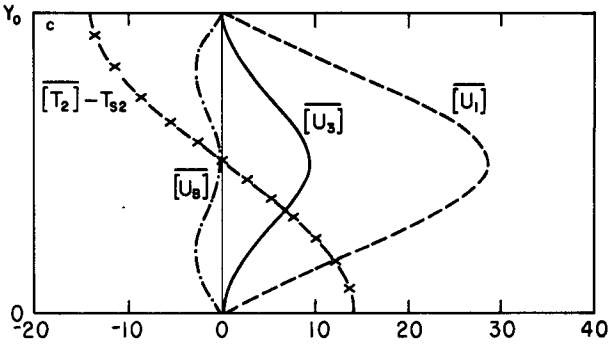

FIG. 5c. As in Fig. 3c except for the quasi-stationary solution.

while the horizontally averaged available potential energy per unit mass is defined by

$$A = \frac{1}{X_0 Y_0} \int_0^{Y_0} \int_0^{X_0} \frac{2}{\Delta p^2 S_p} \phi_S^2 dxdy. \tag{14}$$

It is easy to prove that the system (5)–(7) conserves the summation of K and A when the heating and friction terms are dropped.

Using the spectral representation for ϕ_M and ϕ_S, Eqs. (13) and (14) become

$$K = \sum_{i=1}^{I} \frac{A_i^2}{f_0^2} (\psi_i^2 + \tau_i^2), \tag{15}$$

$$A = \sum_{i=1}^{I} \frac{2}{\Delta p^2 S_p} \tau_i^2. \tag{16}$$

Here I is an integer where we truncate the spectral expansion.

In our consideration of the energy balance, we are concerned with the kinetic energy and the available potential energy of time-averaged zonal mean flow (K_Z and A_Z), of time-averaged eddies (K_S and A_S) and of transient flow (K_T and A_T), so that

$$\bar{K} = K_Z + K_S + K_T, \tag{17}$$

$$\bar{A} = A_Z + A_S + A_T, \tag{18}$$

where the overbar represents the time-averaging operator. If we let square brackets be the zonal averaging operator and let the asterisk represent the deviation from the zonal mean, then for a variable Z, $[\bar{Z}]$ is its time-averaged zonal mean, $\bar{Z}^*$ its time-averaged eddy and $Z' = Z - [\bar{Z}] - \bar{Z}^* = Z - \bar{Z}$ its transient eddy. We can derive the following energy equations:

$$\frac{dK_Z}{dt} = -C(K_Z,K_S) - C(K_Z,K_T) + C(A_Z,K_Z) - CB(K_Z,K_S) - CB(K_Z,K_T) - D_Z, \tag{19}$$

$$\frac{dK_S}{dt} = C(K_Z,K_S) - C(K_S,K_T) + C(A_S,K_S) + CB(K_Z,K_S) - D_S, \tag{20}$$

$$\frac{dK_T}{dt} = C(K_Z,K_T) + C(K_S,K_T) + C(A_T,K_T) + CB(K_Z,K_T) - D_T, \tag{21}$$

$$\frac{dA_Z}{dt} = -C(A_Z,K_Z) - C(A_Z,A_S) - C(A_Z,A_T) + G_Z, \tag{22}$$

$$\frac{dA_S}{dt} = -C(A_S,K_S) + C(A_Z,A_S) - C(A_S,A_T) + G_S, \tag{23}$$

$$\frac{dA_T}{dt} = -C(A_T,K_T) + C(A_Z,A_T) + C(A_S,A_T) + G_T. \tag{24}$$

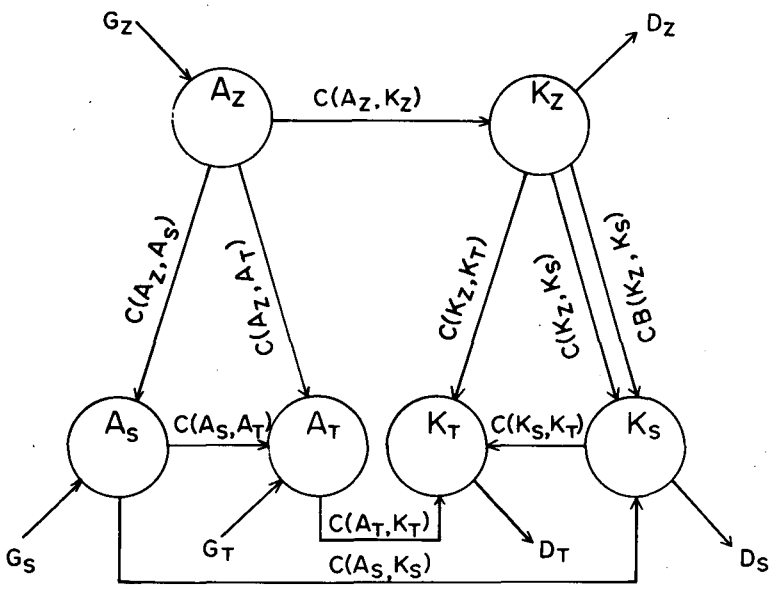

FIG. 6. Energy cycle diagram. The arrows indicate the positive direction of individual processes as defined by Eqs. (A1)–(A17).

The definition of each term on the right-hand side of (19)–(24) is given in the Appendix. Symbolically, $C(A,B)$ means conversion of A to B, G_T means generation of A_T, and D_T means dissipation of K_T.

If we drop the diabatic heating and dissipation terms from Eqs. (19)–(24) and then take the sum of these equations, we obtain

$$\frac{d}{dt}(K_Z + K_S + K_T + A_Z + A_S + A_T) = 0. \quad (25)$$

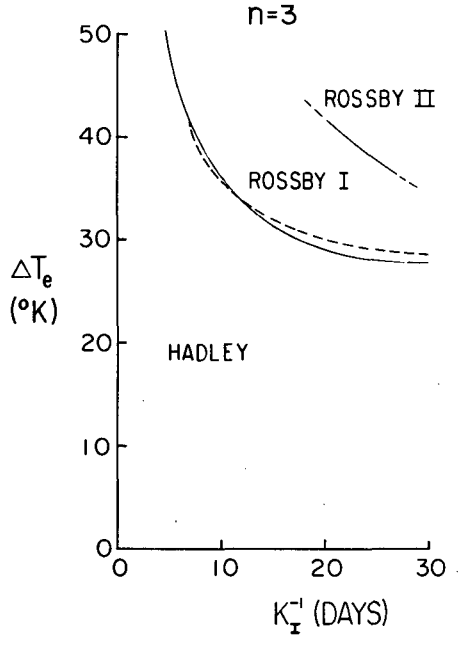

FIG. 7. Stability diagram for the case $n = 3$.

Therefore, the truncated spectral model still conserves the sum of total kinetic and available potential energy.

Fig. 6 shows the energy exchange processes in an energy cycle diagram. The arrows indicate the direction of the energy conversions when (A1)–(A17) are positive. In addition to the cycle $A_Z \rightarrow A_T \rightarrow K_T \rightarrow K_Z$, the cycle $A_Z \rightarrow A_S \rightarrow K_S \rightarrow K_Z$ is shown. These two cycles interact through energy conversions between A_S and A_T, between K_S and K_T, and between A_Z and K_Z. $CB(K_Z,K_S)$ and $CB(K_Z,K_T)$ are energy conversions due to the topographical effect. This topographical effect is in the form of a vertical geopotential flux at the surface. $CB(K_Z,K_T)$ is usually negligible, and so is not shown in the figure. The processes $C(A_Z,A_S)$ and $C(K_Z,K_S)$ are similar to the processes $C(A_Z,A_T)$ and $C(K_Z,K_T)$, but associated with the quasi-stationary eddies. The processes $C(A_Z,A_S)$ and $C(K_Z,K_S)$ will be triggered if there is topography because of the presence of damping mechanisms.

a. Case n = 3

Fig. 7 is the stability diagram for $n = 3$. The solid curve describing the transition between the Hadley and the Rossby regimes is obtained by a stability study (Yao, 1977). In the Hadley regime there are stationary waves plus zonal mean flow. This combined flow is stable with respect to perturbations, and therefore is still regarded as in the Hadley regime even though there are eddies included. There is no "upper" Hadley regime, because the static stability is assumed a constant.

In the Rossby regime the zonal mean flow and/or stationary waves are unstable with respect to perturbations. The dashed curve close to the solid curve describes the transition between the Hadley and the Rossby regimes in the case of no topography. It is apparent that topography has little effect on the stability properties of the zonal mean flow. The linear baroclinic stability properties of a two-level quasi-geostrophic atmosphere on a β-plane has been discussed by Phillips (1954).

In Fig. 7 there is a curve which denotes the transition between two Rossby regimes, I and II. In the Rossby regime I, the energetics of the quasi-stationary waves is basically the same as the energetics of the stationary waves in the Hadley regime. The kinetic energy (K_S) is maintained mainly by the topographical forcing, whereas in the Rossby regime II, K_S is maintained mainly through the energy conversion $A_S \rightarrow K_S$. In all three regimes, the available potential energy of the quasi-stationary waves (A_S) is maintained by the energy conversion $A_Z \rightarrow A_S$. When ΔT_e or k_I^{-1} is sufficiently large, the model's motion becomes highly irregular and a clear distinction between different Rossby regimes can not be made. However, when ΔT_e or k_I^{-1} is very large, the assumption of a constant static stability must be highly unsatisfactory.

As an example from Rossby regime II, Fig. 8 shows the time-averaged energy cycle diagram from the results of integration for the combination $\Delta T_e = 38$ K and $k_I^{-1} = 26$ days. We see that the transient waves are essentially maintained by the baroclinic instability of the mean flow. The transient waves feed part of their kinetic energy back to the kinetic energy of the zonal mean flow through the barotropic processes. The above energy cycle is typical of the atmosphere (cf. Oort, 1964) and is clearly produced by our model.

The available potential energy A_S of the quasi-stationary waves is maintained by the energy conversion $A_Z \rightarrow A_S$. A portion of A_S is then converted to the kinetic energy K_S of quasi-stationary waves; K_S is also produced from the conversion $K_Z \rightarrow K_S$ through the topographical effect. However, a portion of K_S feeds back to the zonal mean flow through the barotropic process associated with momentum transports. It is seen that $C(A_S,K_S)$ is considerably larger than $CB(K_Z,K_S)$. From this we conclude that the kinetic energy of the quasi-stationary waves for this case is maintained mainly by the energy conversion $A_S \rightarrow K_S$. This result is similar to the findings of Holopainen (1970) for winter.

The time-averaged values of energy conversion between A_S and A_T and energy conversion between K_S and K_T are relatively small. However, in examining the time series of energy conversion associated with the transient waves (Fig. 9) we see that the conversion process $C(K_S,K_T)$ is quite large instantaneously. It follows, then, that the barotropic instability of quasi-stationary waves is quite significant over shorter periods. However, the process $C(A_S,A_T)$ is very small all the time.

From Fig. 9 we also see that $C(K_Z,K_T)$ is oscillatory in time with quite a large magnitude. The

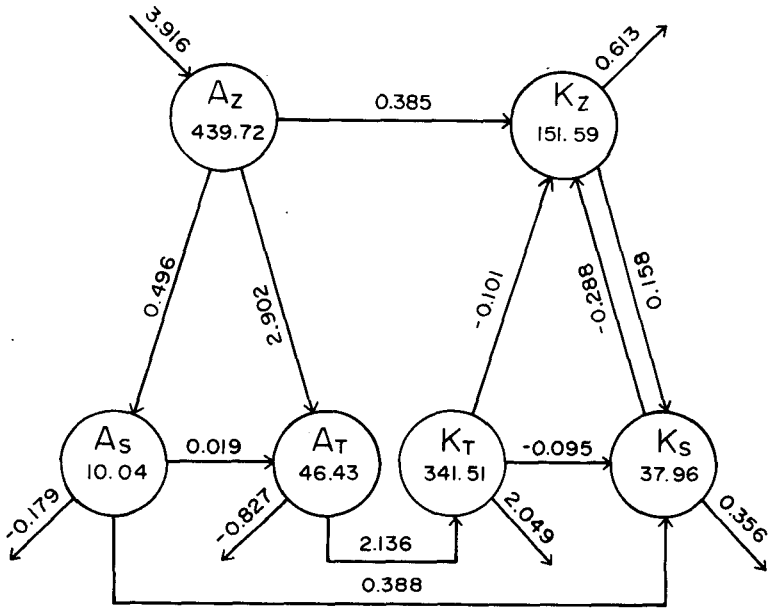

FIG. 8. Energy cycle of the quasi-steady state with $n = 3$, $k_I^{-1} = 26$ days and $\Delta T_e = 38$ K. Energy is in units of $m^2\ s^{-2}$, while conversion rates are in units of $10^{-4} \times m^2\ s^{-3}$.

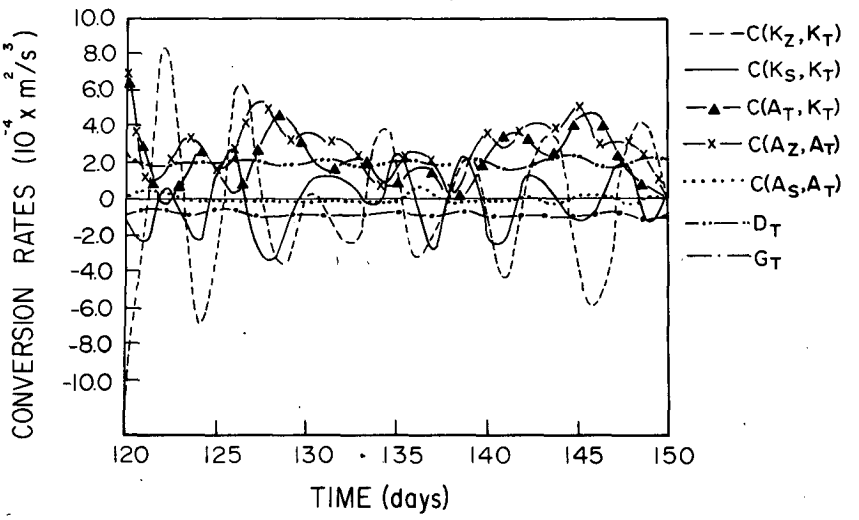

FIG. 9. Time series of the energy conversion rates for $n = 3$ with $k_I^{-1} = 26$ days and $\Delta T_e = 38$ K. The thin solid line is a reference line where conversion rates are zero.

oscillation of $C(K_Z,K_T)$ is a manifestation of the barotropic cycle [cf. Arakawa, (1961) and Thompson (1957)]. The conversions $C(A_Z,A_T)$ and $C(A_T,K_T)$ are large and usually positive. The oscillations of $C(A_Z,A_T)$ and $C(A_T,K_T)$ are manifestations of the baroclinic cycle (cf. Pedlosky, 1970, 1971, 1972).

As an example from Rossby regime I, Fig. 10 shows the energy cycle diagram for the combination of $k_I^{-1} = 26$ days and $\Delta T_e = 34$ K. We see that the major features of the energy cycle associated with the transient waves are the same as before. However, it is apparent in this case that the quasi-stationary waves are maintained by the topographical effect $CB(K_Z,K_S)$, rather than by the conversion $C(A_S,K_S)$. The conversions $C(K_S,K_T)$ and $C(A_S,A_T)$ are small even instantaneously.

A different kind of behavior occurs when ΔT_e or k_I^{-1} is sufficiently large. Under these circumstances, the motion is highly irregular. The values of $C(A_S,A_T)$ and $C(K_S,K_T)$ can be very large.

In order to understand the physical processes responsible for maintaining the quasi-stationary

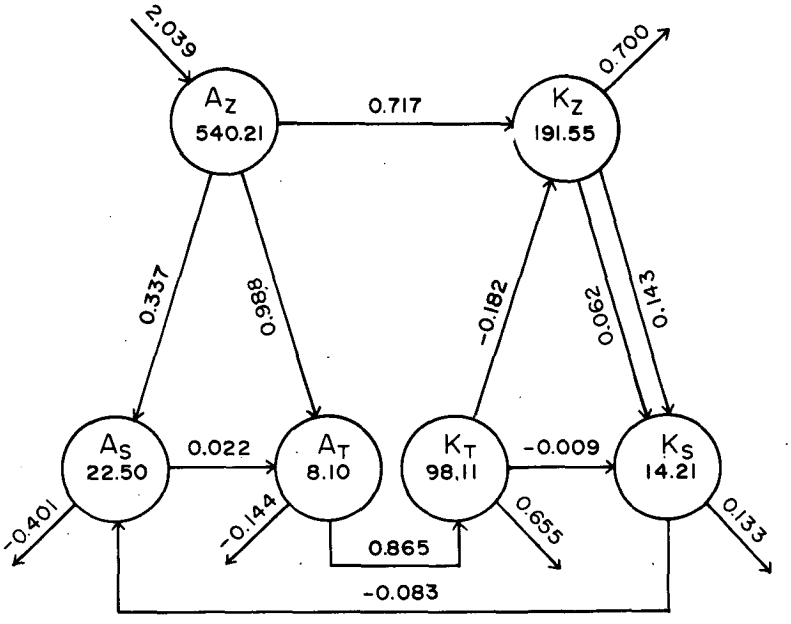

FIG. 10. As in Fig. 8 except with $\Delta T_e = 34$ K.

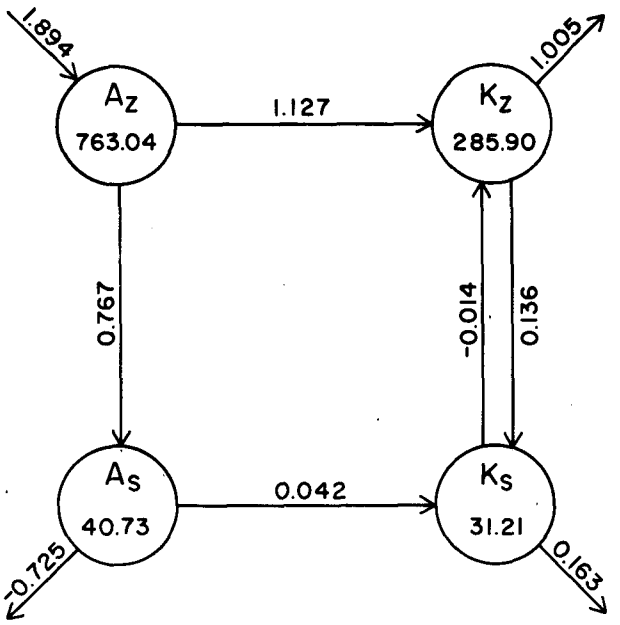

FIG. 11. Energy cycle of the stationary solution with $n = 3$, $k_I^{-1} = 26$ days and $\Delta T_e = 38$ K.

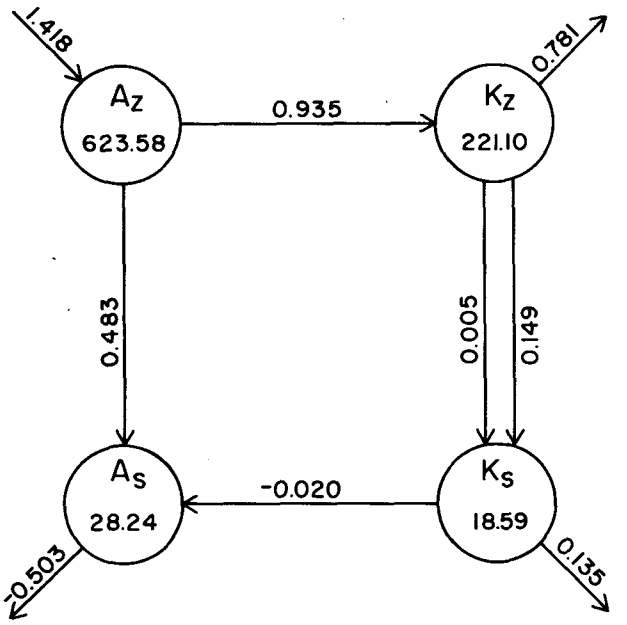

FIG. 12. As in Fig. 11 except with $\Delta T_e = 34$ K.

waves in Rossby regime II, we will also look into the energy spectra and energetics of the stationary solutions for some selected cases.

Figs. 11 and 12 show the energetics diagrams for the stationary solutions with the combinations of $k_I^{-1} = 26$ days and $\Delta T_e = 38$ K (Fig. 11) and $k_I^{-1} = 26$ days and $\Delta T_e = 34$ K (Fig. 12). Comparing Figs. 12 and 10, we see that in Rossby regime I, the energetics of the stationary waves is little influenced by the presence of baroclinic waves. Thus, the quasi-statonary solution is similar to the stationary solution (cf. Figs. 3 and 5). In Rossby regime II (cf. Figs. 11 and 8), there is a large loss of stationary eddy available potential energy because of the quasi-stationary baroclinic eddies drawing on that energy source. Comparing Figs. 4 and 2, we see that the higher modes have larger amplitude in the quasi-stationary waves. This meridional structure makes it more efficient for the baroclinic eddies to draw energy from the forced waves, because the zonal perturbation velocity and the associated zonal heat fluxes are maximized.

Table 1 shows the energy spectra for three selected cases. For $n = 3$, $k_I^{-1} = 26$ days and $\Delta T_e = 34$ K, the dominant wavenumbers are well separated between quasi-stationary waves and transient eddies. It is apparent that the dominant quasi-stationary

TABLE 1. Energy spectra of three selected cases.*

n	$(k_I^{-1}, \Delta T_e)$	K_Z	K_S		K_T			A_Z	A_S			A_T	
			K_{S1}	K_{S2}	K_{T0}	K_{T1}	K_{T2}		A_{S1}	A_{S2}	A_{T0}	A_{T1}	A_{T2}
3	(26,38)	151.66	37.81		341.10			440.30	9.85			46.34	
			36.58	1.23	26.20	62.12	252.77		9.63	0.22	4.02	10.85	31.47
3	(26,34)	191.54	14.20		98.13			540.20	22.50			8.11	
			14.17	0.03	0.00	0.40	97.73		22.49	0.01	0.00	0.13	7.97
2	(26,38)	299.79	8.18		84.02			668.92	23.43			22.23	
			7.93	0.25	0.91	0.83	82.27		23.36	0.07	0.20	0.35	21.67

* Energy is in the unit $m^2\ s^{-2}$. The subscripts 0, 1 and 2 denote the energy components of wavenumbers 0, n and $2n$, respectively. The numbers shown in this table are very slightly different from the Figs. 8, 10 and 14, because of redoing numerical integration and energetics analyses with a different computer at GISS.

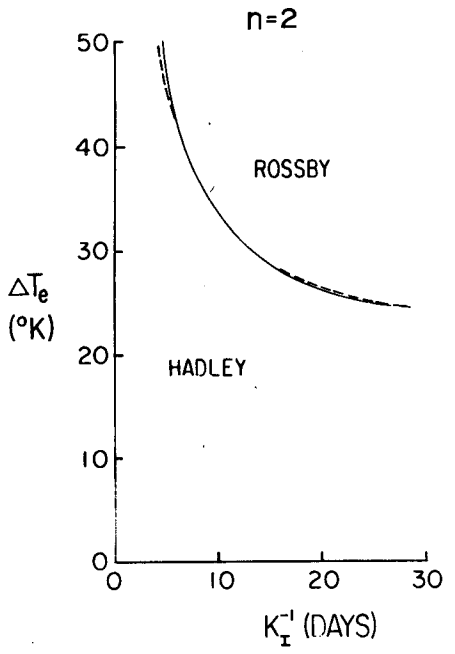

FIG. 13. Stability diagram for the case $n = 2$.

wave is wavenumber 3 and is forced by the topography, and that the dominant transient wave is wavenumber 6 and is due to baroclinic instability of the zonal mean flow. For $\Delta T_e = 38$ K, wavenumber 3 is also unstable baroclinically. There are two energy sources for this baroclinic wave—one is the zonal mean flow, the other the forced waves. Thus, the baroclinic wave of wavenumber 3 consists of two components (which may not be well separated): one component draws energy from the zonal mean flow and tends to be traveling and have larger wavelength in the meridional direction; the other component draws energy from the forced waves and tends to be stationary and have shorter wavelength in the meridional direction. As a result, both the quasi-stationary and transient eddy components are enhanced. This mechanism of cooperation between forcing and baroclinic instability appears to be largely responsible for the maintenance of the quasi-stationary waves in Rossby regime II. This mechanism disappears if there is no topography. Topography not only triggers the generation of eddy available potential energy, but also serves as a phase fixing mechanism.

b. Case n = 2

Fig. 13 is the stability diagram for $n = 2$. The curve denoting the transition between the Hadley and Rossby regimes is obtained as before. However, a delineation between different Rossby regimes cannot be defined unambiguously. For relatively small values of ΔT_e and k_I^{-1}, typical of the atmospheric values, K_S of the quasi-stationary waves in the Rossby regime is maintained by the topographical forcing whereas A_S is maintained by the energy conversion $A_Z \rightarrow A_S$. When ΔT_e or k_I^{-1} is sufficiently large, the motion becomes highly irregular, and no single kind of behavior is observed.

As an example of the cases with relatively small ΔT_e and k_I^{-1}, Fig. 14 shows the energy cycle diagram for the combination $\Delta T_e = 38$ K and $k_I^{-1} = 26$ days. We see that the energy cycle for transient waves is basically the same as it was for $n = 3$. K_S, however, is no longer maintained by the energy conversion $A_S \rightarrow K_S$. Topographical forcing is the mechanism mainly responsible for maintaining the quasi-sta-

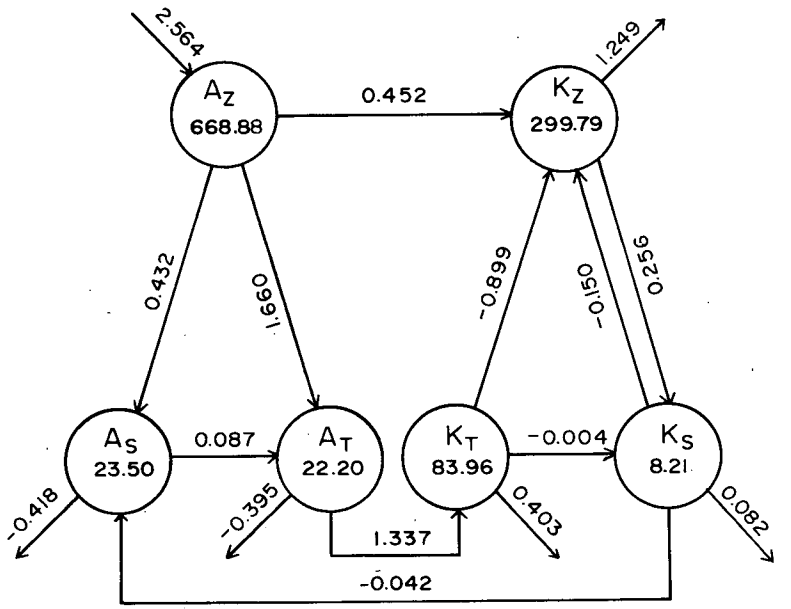

FIG. 14. As in Fig. 8 except with $n = 2$.

tionary waves. Interactions between transient and quasi-stationary waves are small even instantaneously (see Fig. 15). On the other hand, the process $C(K_Z,K_T)$ is significant and is consistently negative, though oscillating in time. $C(A_Z,A_T)$ and $C(A_T,K_T)$ have large positive values. Therefore, barotropic and baroclinic oscillations are both produced in this case. Once again, the interactions between transient and quasi-stationary waves can be very large if motion is in the highly irregular regime.

Table 1 also shows the energy spectra for the case k_I^{-1} = 26 days and ΔT_e = 38 K with n = 2. It is clear that for this case the physical processes are very similar to the case with k_I^{-1} = 26 days and ΔT_e = 34 K when n = 3 in Rossby regime I.

5. Summary and conclusions

In summary, a truncated two-level quasi-geostrophic spectral model in a zonal channel on a beta-plane was developed to study the maintenance of the quasi-stationary waves forced by topography. The model's motion contains wavenumbers 0, n and $2n$ in the zonal direction, where n is the lowest eddy wavenumber as well as the wavenumber of the topography. The first three modes in the meridional direction are allowed for each wave. The study covered the two cases defined by n = 2 and n = 3.

The spectral model was integrated by initially perturbing the stationary solution of the equations governing the spectral coefficients. A detailed energetics study was made of the quasi-equilibrium state to study the maintenance of the quasi-stationary waves.

If the flow is not highly irregular, the available potential energy of quasi-stationary waves is maintained by the energy conversion $A_Z \rightarrow A_S$. For n = 3 and moderately large ΔT_e and k_I^{-1}, the kinetic energy of these waves is maintained by the energy conversion $A_S \rightarrow K_S$. If ΔT_e or k_I^{-1} is smaller while n = 3, kinetic energy is supplied to the quasi-stationary waves by the energy conversion $K_Z \rightarrow K_S$ through the topographic effect in the form of a vertical geopotential flux at the surface. The latter mechanism also maintains the kinetic energy of the quasi-stationary waves for n = 2 with relatively small ΔT_e and k_I^{-1}. When ΔT_e or k_I^{-1} is sufficiently large, a unique Rossby regime cannot be defined for either n = 2 or n = 3.

The findings that quasi-stationary waves are maintained by energy conversions $A_Z \rightarrow A_S$ and $A_S \rightarrow K_S$ when n = 3 in Rossby regime II implies that these quasi-stationary waves are generated mainly by baroclinic instability of the forced waves. This kind of baroclinic wave tends to become stationary in order to draw efficiently on the available energy of the forced wave. According to Stone (1977) such a cooperation between forcing and baroclinic instability is a plausible explanation of the baroclinic nature of the quasi-stationary waves as observed by Halopainen (1970) in winter. In summer, when the meridional temperature gradient is small, the atmospheric circulation would be in Rossby regime I.

The oscillation of $C(K_S,K_T)$ has apparently not been found before. This oscillation tells us that there is an energy conversion oscillation between K_S and K_T. The behavior of the atmospheric circulation associated with this oscillation requires further study.

In order to see whether the results associated with n = 3 are due to too much forcing when 750 m is used as the topographic amplitude, calculations were also made for n = 3 with 500 m as the

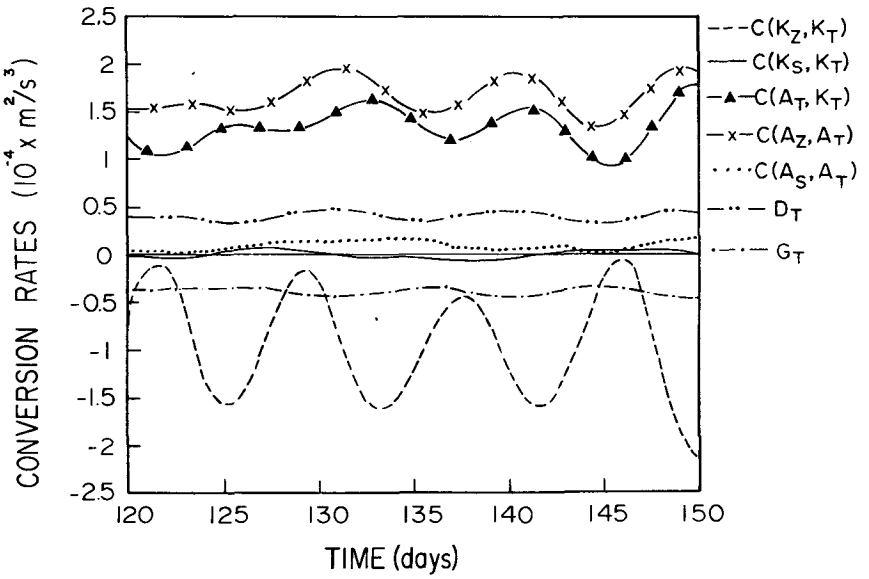

FIG. 15. As in Fig. 9 except with n = 2.

topographic amplitude for some selected combinations of ΔT_e and k_I^{-1}. The amplitude of the earth's topography at 30°N for $n = 3$ is about 500 m. The results obtained for this choice of topographic amplitude showed similar features to the case in which 750 m was used.

The forcing effect of stationary heat sources and sinks was not considered here, and therefore we do not seriously compare results obtained here with observations. As is known, this thermal forcing is another major mechanism in producing quasi-stationary waves in the atmosphere (e.g., Derome and Wiin-Nielsen, 1971), and is particularly important in summer (Holopainen, 1970). We plan to conduct future studies similar to the one described here but including the thermal forcing by stationary heat sources and sinks.

The truncation of the spectral model restricts the production of transient waves. Experiments with more degrees of freedom would also be a worthwhile extension of this study.

Acknowledgments. The paper reported here is an extension from the author's Ph.D. dissertation (Yao, 1977). He is indebted to Professor Akio Arakawa of the University of California, Los Angeles, for his guidance through that dissertation work.

Thanks are due to Drs. J. Hansen of Goddard Institute for Space Studies and P. Stone of M.I.T. for their useful comments and reviewing the manuscript.

This research was supported in part by the National Science Foundation under Grant ATM 7201502 and by the National Aeronautics and Space Administration under Grant NGR 05007328.

APPENDIX

The Definition of Energy Conversion and Sink Source Terms

The energy conversion terms and sink and source terms on the right hand side of Eqs. (19)–(24) are defined as follows:

$$C(K_Z,K_S) = -\sum_{i=1}^{M-1}\frac{2\bar{\psi}_i}{f_0^3}\Big[\sum_{j<k=1}^{I}(A_j^2 - A_k^2)C_{ijk}(\bar{\psi}_j\bar{\psi}_k + \bar{\tau}_j\bar{\tau}_k)\Big] - \sum_{i=1}^{M-1}\frac{2\bar{\tau}_i}{f_0^3}\Big[\sum_{j<k=1}^{I}(A_j^2 - A_k^2)C_{ijk}(\bar{\tau}_j\bar{\psi}_k + \bar{\psi}_j\bar{\tau}_k)\Big] \quad \text{(A1)}$$

$$C(K_Z,K_T) = -\sum_{i=1}^{M-1}\frac{2\bar{\psi}_i}{f_0^3}\Big[\sum_{j<k=1}^{I}(A_j^2 - A_k^2)C_{ijk}(\overline{\psi_j'\psi_k'} + \overline{\tau_j'\tau_k'})\Big] - \sum_{i=1}^{M-1}\frac{2\bar{\tau}_i}{f_0^3}\Big[\sum_{j<k=1}^{I}(A_j^2 - A_k^2)C_{ijk}(\overline{\tau_j'\psi_k'} + \overline{\psi_j'\tau_k'})\Big] \quad \text{(A2)}$$

$$C(K_S,K_T) = -\sum_{i=M}^{I}\frac{2\bar{\psi}_i}{f_0^3}\Big[\sum_{j<k=1}^{I}(A_j^2 - A_k^2)C_{ijk}(\overline{\psi_j'\psi_k'} + \overline{\tau_j'\tau_k'})\Big] - \sum_{i=M}^{I}\frac{2\bar{\tau}_i}{f_0^3}\Big[\sum_{j<k=1}^{I}(A_j^2 - A_k^2)C_{ijk}(\overline{\tau_j'\psi_k'} + \overline{\psi_j'\tau_k'})\Big] \quad \text{(A3)}$$

$$C(A_Z,K_Z) = -\sum_{i=1}^{M-1}\frac{2\bar{\tau}_i}{\Delta p}\bar{W}_i \quad \text{(A4)}$$

$$C(A_S,K_S) = -\sum_{i=M}^{I}\frac{2}{\Delta p}\bar{\tau}_i\bar{W}_i \quad \text{(A5)}$$

$$C(A_T,K_T) = -\sum_{i=1}^{I}\frac{2}{\Delta p}\overline{\tau_i'W_i'} \quad \text{(A6)}$$

$$C(A_Z,A_s) = -\sum_{i=1}^{M-1}\frac{4\bar{\tau}_i}{\Delta p^2 S_p f_0}\sum_{j<k=1}^{I}C_{ijk}(\bar{\tau}_j\bar{\psi}_k - \bar{\psi}_j\bar{\tau}_k) \quad \text{(A7)}$$

$$C(A_Z,A_T) = -\sum_{i=1}^{M-1}\frac{4\bar{\tau}_i}{\Delta p^2 S_p f_0}\sum_{j<k=1}^{I}C_{ijk}(\overline{\tau_j'\psi_k'} - \overline{\psi_j'\tau_k'}) \quad \text{(A8)}$$

$$C(A_S,A_T) = -\sum_{i=1}^{I}\frac{4\bar{\tau}_i}{\Delta p^2 S_p f_0}\sum_{j<k=1}^{I}C_{ijk}(\overline{\tau_j'\psi_k'} - \overline{\psi_j'\tau_k'}) \quad \text{(A9)}$$

$$CB(K_Z,K_S) = \frac{2\epsilon}{f_0^2} \sum_{i=M}^{I} (\bar{\tau}_i - \bar{\psi}_i) \sum_{j<k=1}^{I} C_{ijk}(H_j\bar{\psi}_{3k} - \bar{\psi}_{3j}H_k) \tag{A10}$$

$$CB(K_Z,K_T) = \frac{2\epsilon}{f_0^2} \overline{[\sum_{i=1}^{I} \tau_i' \sum_{j<k=1}^{I} C_{ijk}(H_j\psi_{3k}' - \psi_{3j}'H_k) - \sum_{i=1}^{I} \psi_i' \sum_{j<k=1}^{I} C_{ijk}(H_j\psi_{3k}' - \psi_{3j}'H_k)]} \tag{A11}$$

$$D_Z = \sum_{i=1}^{M-1} \frac{k_B}{f_0^2} A_i^2\bar{\psi}_i\bar{\psi}_{Bi} - \sum_{i=1}^{M-1} \frac{2A_i^2}{f_0^2} \bar{\tau}_i(\tfrac{1}{2}k_B\bar{\psi}_{Bi} - 2k_I\bar{\tau}_i) \tag{A12}$$

$$D_S = \sum_{i=M}^{I} \frac{k_B}{f_0^2} A_i^2\bar{\psi}_i\bar{\psi}_{Bi} - \sum_{i=M}^{I} \frac{2A_i^2}{f_0^2} \bar{\tau}_i(\tfrac{1}{2}k_B\bar{\psi}_{Bi} - 2k_I\bar{\tau}_i) \tag{A13}$$

$$D_T = \sum_{i=1}^{I} \frac{k_B}{f_0^2} A_i^2\overline{\psi_i'\psi_{Bi}'} - \sum_{i=1}^{I} \frac{2A_i^2}{f_0^2} \overline{\tau_i'(\tfrac{1}{2}k_B\psi_{Bi}' - 2k_I\tau_i')} \tag{A14}$$

$$G_Z = \sum_{i=1}^{M-1} \frac{4\mu}{\Delta p^2 S_p} \bar{\tau}_i(\tau_{ei} - \bar{\tau}_i) \tag{A15}$$

$$G_S = -\sum_{i=M}^{I} \frac{4\mu}{\Delta p^2 S_p} \bar{\tau}_i\bar{\tau}_i \tag{A16}$$

$$G_T = -\sum_{i=1}^{I} \frac{4\mu}{\Delta p^2 S_p} \overline{\tau_i'\tau_i'}. \tag{A17}$$

Here M is an integer such that F_i for any $i < M$ has no zonal variation and F_i for $i \geq M$ always has zonal variation. A_i^2 is defined by

$$\nabla^2 F_i = -A_i^2 F_i, \qquad i = 1, 2, 3, \ldots .$$

REFERENCES

Arakawa, A., 1961: The variation of general circulation in the barotropic atmosphere. *J. Meteor. Soc. Japan*, **39**, 49–58.

Bolin, B., 1950: On the influence of the earth's orography on the general character of the westerlies. *Tellus*, **2**, 184–195.

Charney, J. G., and A. Eliassen, 1949: A numerical method for predicting the perturbations of the middle latitude westerlies. *Tellus*, **1**, 38–54.

——, and P. G. Drazin, 1961: Propagation of planetary-scale disturbances from the lower into the upper atmosphere. *J. Geophys. Res.*, **66**, 83–109.

——, and J. G. DeVore, 1979: Multiple flow equilibria in the atmosphere and blocking. *J. Atmos. Sci.*, **36**, 1205–1216.

Derome, J., and A. Wiin-Nielsen, 1971: The response of a middle-latitude model atmosphere to forcing by topography and stationary heat sources. *Mon.Wea. Rev.*, **99**, 564–576.

Eliassen, A., and E. Palm, 1961: On the transfer of energy in stationary mountain waves. *Geofys. Publ.*, **22**, No. 3.

Gambo, K., 1956: The topographical effects upon the jet stream in the westerlies. *J. Meteor. Soc. Japan*, **34**, 34–38.

Holopainen, E. O., 1966: A diagnostic study of the maintenance of stationary disturbances in the atmosphere. Tech. Rep. No. 3, Dept. Meteor. Oceanogr., University of Michigan, 40 pp.

——, 1970: An observational study of the energy balance of the stationary disturbances in the atmosphere. *Quart. J. Roy. Soc.*, **96**, 626–644.

Lorenz, E. N., 1963: The mechanics of vacillation. *J. Atmos. Sci.*, **20**, 448–464.

Matsuno, T., 1970: Vertical propagation of stationary planetary waves in the winter Northern Hemispheres. *J. Atmos. Sci.*, **27**, 871–883.

Murakami, T., 1963a: On the maintenance of kinetic energy of the large-scale stationary disturbances in the atmosphere. Final Report on Planetary Circulation Project, Dept. of Meteorology, MIT, 42 pp.

——, 1963b: The topographic effects in three-level model of the s-coordinate. *Pap. Meteor. Geophys.*, **14**, Tokyo, 144–150.

Newton, C. W., 1971: Mountain torques in the global angular momentum balance. *J. Atmos. Sci.*, **28**, 623–628.

Oort, A. H., 1964: On estimates of the atmospheric energy cycle. *Mon. Wea. Rev.*, **92**, 483–493.

Pedlosky, J., 1970: Finite-amplitude baroclinic waves. *J. Atmos. Sci.*, **27**, 15–30.

——, 1971: Finite-amplitude baroclinic waves with small dissipation. *J. Atmos. Sci.*, **28**, 587–597.

——, 1972: Limit cycles and unstable baroclinic waves. *J. Atmos. Sci.*, **29**, 53–63.

Phillips, N. A., 1954: Energy transformation and meridional circulations associated with simple baroclinic waves in a two-level quasi-geostrophic model. *Tellus*, **3**, 273–286.

Saltzman, B., 1968: Surface boundary effects on the general circulation and macroclimate: A review of the theory of quasi-stationary perturbation in the atmosphere. *Meteor. Monogr.*, No. 30, 4–19.

Stone, P. H., 1977: Generation of atmospheric eddies. *Investigations of the Synoptic Variability of the Ocean*, Academy of Sciences of the Uk.S.S.R., Sevastopol, V. M. Kamenovich and P. B. Rhines, Ed., 400–421.

Thompson, P. D., 1957: A heuristic theory of large-scale turbulence and long-period velocity variations in barotropic flow. *Tellus*, **9**, 69–91.

White, R. M., 1949: The role of the mountains in the angular momentum balance of the atmosphere. *J. Meteor.*, **6**, 353–355.

Yao, M.-S., 1977: Thermally and topographically forced general circulation regimes of a two-level quasi-geostrophic atmosphere. Ph.D. thesis, University of California, 161 pp.